

NUMERICAL INVESTIGATION OF BEAM HALO FROM BEAM GAS SCATTERING IN KEK-ATF*

R. Yang[†], P. Bambade, LAL, Univ. Paris-Sud, CNRS/IN2P3, Université Paris-Saclay, Orsay, France
K. Kubo, T. Okugi, N. Terunuma, D. Zhou, KEK and SOKENDAI, Tsukuba, Japan

Abstract

To demonstrate the final focus schemes of the Future Linear Collider (FLC), the Accelerator Test Facility 2 (ATF2) at KEK is devoted to focus the beam to a RMS size of a few tens of nanometers (nm) vertically and to provide stability at the nm level at the virtual Interaction Point (IP). However, the loss of halo particles upstream will introduce background to the diagnostic instrument measuring the ultra-small beam, using a laser interferometer monitor. To help the realization of the above goals and beam operation, understanding and mitigation of beam halo are crucial. In this paper, we present the systematical simulation of beam halo formation from beam gas Coulomb scattering (BGS) in the ATF damping ring. The behavior of beam halo with various machine parameters is also discussed.

INTRODUCTION

As a test beam line for the Final Focus Systems based on the local chromaticity correction scheme, ATF2 aims to achieve a 37 nm vertical beam size at the virtual Interaction Point (IP), with a stability at the nm level [1, 2]. To visualize the vertical spot size at the IP, a laser interferometer monitor, *Shintake Monitor*, was installed [3]. Beam size is measured from the modulation of the Compton scattering signal. Accuracy reconstruction of this modulation can be affected by background caused by loss of halo particles upstream.

Beam gas Coulomb scattering (BGS), Intra-Beam Scattering (IBS) and the residual alignment errors are considered the main sources of beam halo in the storage ring. Besides, optical mismatch and the wakefield effects in the ATF2 beam line can also contribute. Considerable efforts have been devoted to revealing the primary halo sources, the main one being BGS, theoretically and experimentally [4–9] (for a recent experimental study, see also Ref. [10]). An analytical method has been established to express the distribution function in the storage ring in the presence of BGS, considered as an incoherent stochastic process [4]. This method has not yet been compared in detail to simulation and measurement.

Accurate and systematic simulation of halo generation is essential to understand the interplay between radiation damping, quantum excitation, residual dispersion, xy coupling and BGS. In this paper, the simulation (based on SAD [11]) of beam halo from BGS in ATF is described, which verifies and complements the analytic estimation.

THEORETICAL APPROXIMATION

Particles are transversely deflected when scattering in the Coulomb field of the nucleus of a residual gas atom, which leads to an increased betatron oscillation amplitude. Considering the optics of the ring in the smooth approximation, Ref. [4] provides an analytical method to approximate the deviation of the beam distribution from a Gaussian shape due to such scatterings. The distribution function in equilibrium is approximated with the scaled single scattering distribution

$$\rho(X) = \int \frac{d\omega}{(2\pi)^2} e^{-i\omega X} \tilde{\psi}_0(\omega) \tilde{\psi}_f(\omega) \quad (1)$$

where X is the normalized coordinate, $X = x/\sigma_x$, $\tilde{\psi}_0(\omega)$ the characteristic function due to synchrotron radiation, $\tilde{\psi}_f(\omega)$ the characteristic function for BGS. $\tilde{\psi}_f(\omega)$ is a function of the scattering rate and of the time over which the evolution of the distribution is considered. Beam profiles can be approximated as Gaussian core plus exponential halo, see Fig.1.

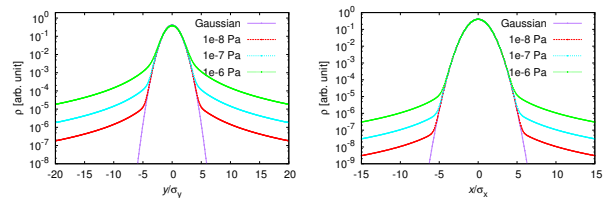


Figure 1: Analytic solution to the beam profile in equilibrium, vertically (left) and horizontally (right).

Here and after, only elastic BGS is taken into account for halo estimation since the probability of inelastic BGS scattering (Bremsstrahlung and inelastic scattering off the e^- of an atom) is 10^{-3} less than elastic scattering in ATF [6].

SIMULATION STUDIES IN ATF

Description of Simulation Method

Tracking of parent and daughter particles is performed turn-by-turn, separately, taking into account synchrotron radiation and quantum excitation. The algorithm adopted to simulate the BGS effect can be summarized as follows: Firstly, in each turn, the number of BGS events is calculated according to the total cross section σ_s and density of gas atoms. The generated events are distributed randomly along the ring. Secondly, the perturbations to the transverse momentum ($\delta x'$, $\delta y'$) of the daughter particles are generated by a Monte-Carlo method according to the cross section. The initial coordinates of the daughter particles are determined by the local Twiss parameters, closed orbit distortion (COD)

* Work supported by Chinese Scholarship Council

[†] ryang@lal.in2p3.fr

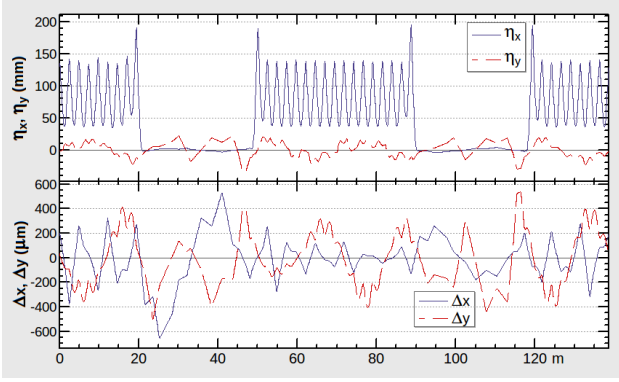


Figure 2: Dispersion functions and COD of ATF ring.

and the beam parameters (taking into account the radiation damping). Thirdly, the scattered particles in the present turn are transported to the observation point, to be combined with the other scattered particles accumulated from the previous turns. The above process is then repeated until extraction.

Equilibrium Parameters

The equilibrium vertical emittance ϵ_y is mainly determined by the residual vertical dispersion η_y and betatron coupling, both of which strongly depend on the residual alignment errors [12]. The vertical emittance which is expected in the presence of realistic residual errors after applying standard corrections is achieved by introducing efficient random vertical displacements to quadrupoles and sextuplets (20 μm and 70 μm , RMS) and rotations to quadrupoles (2 mrad, RMS). The residual COD following this procedure is less than 600 μm , while η_y is under 30 mm, as shown in Fig.2. The equilibrium emittance ϵ_y , obtained for various seeds, ranges from 5 pm to 30 pm, as shown in Table 1.

Table 1: ATF beam parameters

Beam energy [GeV]	E_0	1.3
Intensity [/pulse]	N	$1\text{-}10 \times 10^9$
Vertical emittance [pm]	ϵ_y	5-30
Horizontal emittance [nm]	ϵ_x	1.17
Energy spread [%]	σ_δ	0.056
Bunch length [mm]	σ_z	5.3
Damping time [ms]	$\tau_x/\tau_y/\tau_z$	27.0/19.8/20.6

Benchmarking of Simulation

Estimation of the vacuum lifetime τ_v , which depends on the BGS directly, supplies a benchmarking of the simulation. Considering the elastic and inelastic scatterings, the theoretical prediction of τ_v can be expressed as

$$\tau_v^{-1} = \rho_v(\sigma_e + \sigma_i)\beta\gamma \quad (2)$$

where ρ_v is the volume density of the residual gas atoms, σ_e and σ_i the cross sections of particles loss due to elastic and inelastic BGS, respectively, β the electron velocity and γ the

Lorentz factor. σ_e is limited by the physical aperture, and σ_i depends on the momentum acceptance ($\sim 1\%$) and the maximum acceptance of the instantaneous orbit. Assuming the residual gas mainly consists of CO and the averaged gas pressure is 1×10^{-6} Pa [13], vacuum lifetime evaluated analytically is 83 min. Meanwhile, the simulated value is 87 min using equilibrium beam parameters and realistic physical apertures [14]. Beam loss due to elastic scattering is more severe than inelastic scattering, by a factor of 2.85, see Fig.3. The former mainly happens in the large β regions, while the latter is concentrated at where η_x is maximal.

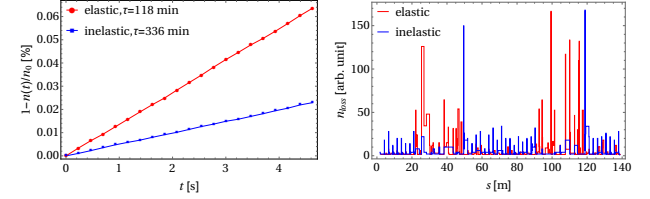


Figure 3: Loss rate (left) and loss map (right) of the scattered particles.

Comparison with Analytic Calculation

Due to the radiation damping, the beam distortion from BGS is mainly determined by the collisions in the time interval just before the extraction. In the theoretical estimation, the distribution is characterized taking into account only scatterings in the last damping time. In the simulation, it takes more than two damping times to obtain the equilibrium distribution, even if differences among profiles for successive damping times are not very large, as shown in Fig.4.

For the typical vacuum level of 5×10^{-7} Pa, satisfactory agreement between the analytical approximation and simulation is observed, see Fig.4, where the distribution is normalized to the RMS beam size. Horizontal tail/halo is lower than vertical halo, by around two orders of magnitude, after such a normalization, due to the large aspect ratio $\epsilon_x/\epsilon_y \approx 100$.

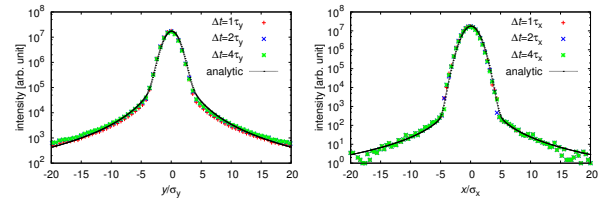


Figure 4: Comparison of vertical (left) and horizontal (right) beam distortion between analytic calculation and simulation.

In the analytic calculation, radiation damping isn't treated dynamically during the considered time interval. Instead, $\tilde{\psi}_0(\omega)$ and $\tilde{\psi}_f(\omega)$ are approximated as being in the final state. Since the distribution function has no assumption whether or not equilibrium has been reached, Eq.(1) can in principle also be used for calculations of the profiles during the damping process. To verify this, beam profiles predicted analytically and by simulation are compared at different times, showing a good agreement, see Fig.5

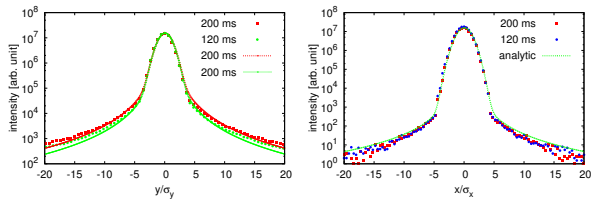


Figure 5: Beam profiles visualized at different moments, vertically (left, symbol:simulation and line:analytic calculation) and horizontally (right, with ϵ_x in equilibrium).

Vacuum Dependence

The probability of BGS is in proportion to the density of residual molecules, and therefore, beam halo varies according to average vacuum in the ring. Presently, the averaged gas pressure is 2×10^{-7} Pa, which can be adjusted by turning on/off part of the ions pumps in the arc section (up to 2×10^{-6} Pa). Simulation is performed for the typical vacuum levels achieved in operation. Significant increases of the beam tail/halo are observed for the worsened vacuum conditions, as shown in Fig.6.

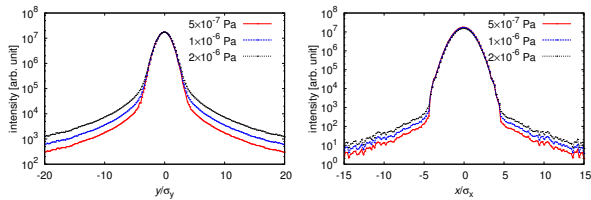


Figure 6: Vacuum dependence of beam halo, vertically (left) and horizontally (right).

Emittance Dependence and Emittance Dilution

Notice that halo from BGS mainly depends on the accumulated stochastic transverse kicks, whereas equilibrium emittance determines beam size (beam core). Therefore, different behaviors of core and halo parts of beam profile due to BGS with various equilibrium emittances are expected. In the physical coordinate system, the beam core is broadened for increasing emittances, while the halo distribution is not affected. An enhancement of beam tail/halo as a function of emittance is therefore observed in the normalized coordinate, see Fig.7. Here, only the evolution with varying ϵ_y is considered since ϵ_y is sensitive to tuning, and halo from BGS is more significant in the vertical plane. The averaged gas pressure is assumed to be 1×10^{-6} Pa. If BGS dominates vertical halo, the relations between emittance and beam tail/halo could be used as an alternative method for vertical ultra-small emittance measurement, without a knowledge of the β value or scanning the betatron phase.

If the BGS rate is large enough, not only halo tails will be produced in the transverse beam distribution, but also some emittance growth can result. With an initial vertical emittance $\epsilon_{y,0} = 12.8$ pm, an increase of 30% for an averaged gas pressure of 5×10^{-6} Pa is found in the simulation. This

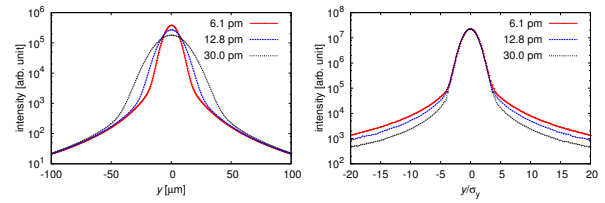


Figure 7: Vertical beam profile with different emittances, in physical frame (left) and the normalized coordinate (right).

exceeds the acceptable value of 10 % [14], but is less than the analytical prediction of 22.8 pm, as shown in Fig.8. We think that this difference arises because radiation damping is not treated as a parallel process in the analytic approximation.

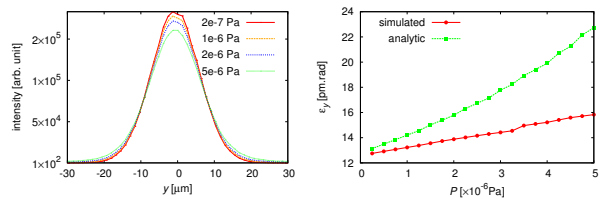


Figure 8: (Left) Vertical distribution for various vacuum levels; (Right) Emittance growth predicted by simulation of scatterings in $4 \tau_y$ and analytic calculation.

CONCLUSION AND PROSPECTS

To understand the generation of beam halo and its dynamics at ATF, a detailed simulation of halo due to BGS was performed. The equilibrium beam parameters are obtained by introducing artificial alignment errors, and the simulation is benchmarked using the vacuum lifetime. Satisfactory agreement between analytical estimations and simulation results of beam halo distributions for different storage time is achieved, which implies the feasibility to extend the convenient analytical approximation along the damping process. Evolution of halo corresponding to various averaged gas pressure is observed, which provides an approach to check if BGS is dominating. Higher tail/halo levels are observed for reduced vertical emittance, for the typical vacuum levels, which indicates a potential model independent to estimate the vertical emittance based on the profile distortion from BGS. The accumulated scatterings can result in some vertical emittance growth for cases of badly deteriorated vacuum levels, however the prediction from simulation and analytical calculation are different, with some improvements apparently needed in the analytical approach. Additional studies are underway, also involving the IBS process, which may play a role in the horizontal halo distribution.

ACKNOWLEDGEMENT

We thank S. Bai, X. Li, T. Naito and K. Oide for helpful discussions, comments and assistance.

REFERENCES

- [1] Grishanov *et al.*, "ATF2 proposal", 2005.
- [2] G. White *et al.*, Experimental validation of a novel compact focusing scheme for future energy-frontier linear lepton colliders, *Rhys. Rev. Lett.* 112, 034802, 2014.
- [3] T. Suehara, *et al.*, "A nanometer beam size monitor for ATF2.", *Nucl. Inst. Meth.*, 616D(1), 2010.
- [4] H. Kohji and K. Yokoya, "Non-Gaussian distribution of electron beams due to incoherent stochastic processes", KEK, 1992.
- [5] T. Raubenheimer, "Emittance growth due to beam-gas scattering", KEK, 1992.
- [6] T. Raubenheimer, "The generation and acceleration of low emittance flat beams for future linear colliders", Standord University, 1991.
- [7] T. Naito and T. Mitsuhashi, "Beam halo measurement utilizing YAG:Ce screen", in *Proc. IBIC'15*, Melbourne, Australia, September 2015, pp. 373-376.
- [8] R. Yang, *et al.*, "Modeling and experimental studies of beam halo at ATF2", in *Proc. IPAC'16*, Busan, Korea, May 2016, p88.
- [9] D. Wang, *et al.*, "Analytical estimation of ATF beam halo distribution." *Chinese physics C* 38.12, 2014.
- [10] R. Yang, *et al.*, "Experimental study of halo formation at ATF2", in *Proc. IPAC'17*, Copenhagen, Denmark, May 2017, MOPAB029.
- [11] SAD is a computer program for accelerator design. <http://acc-physics.kek.jp/SAD/sad.html>
- [12] T. Raubenheimer, *et al.*, "The vertical emittance in the ATF damping ring.", *Nucl. Inst. Meth.* A335, 1993.
- [13] T. Okugi, *et al.*, "Evaluation of vertical emittance in KEK-ATF by utilizing lifetime measurement", *Nucl. Inst. Meth.* A455(1), 2000.
- [14] F. Hinode, *et al.* "ATF Design and Study report." KEK Internal 95.4, 1995.